International Journal of Concrete Structures and Materials

RESEARCH

Open Access

Experiment and Analysis of Mechanical Properties of Lightweight Concrete Prefabricated Building Structure Beams

Yingguang Fang[1], Yafei Xu[1] and Renguo Gu[1,2*]

Abstract

Recent years have witnessed that the prefabricated concrete structure is in the widespread use of building structures. This structure, however, still has some weaknesses, such as excessive weight of components, high requirements for construction equipment, difficult alignment of nodes, and poor installation accuracy. In order to handle the problems mentioned above, the prefabricated component made of lightweight concrete is adopted. At the same time, this prefabricated component is beneficial to reducing the load of the building structure itself and improving the safety and economy of the building structure. Nevertheless, it is rarely found that the researches and applications of lightweight concrete for stressed members are conducted. In this context, this paper replaces ordinary coarse aggregate with lightweight ceramsite or foam based on the C60 concrete mix ratio so as to obtain a mix ratio of C40 lightweight concrete that meets the engineering standards. Besides, ceramsite concrete beams and foamed concrete beams are fabricated. Moreover, through three-point bending tests, this paper further explores the mechanical properties of lightweight concrete beams and plain concrete beams during normal use conditions. As demonstrated in the results, the mechanical properties of the foamed concrete beam are similar to those of the plain concrete beam. Compared to plain concrete beams, the density of foamed concrete beams was lower by 23.4%; moreover, the ductility and toughness of foamed concrete were higher by 13% and 3%, respectively. However, in comparison with the plain concrete beam, the mechanical properties of the ceramsite concrete beam have some differences, with relatively large dispersion and obvious brittle failure characteristics. Moreover, in consideration of the nonlinear deformation characteristics of reinforced concrete beams, the theoretical calculation value of beam deflection was given in this paper based on the assumption of flat section and the principle of virtual work. The theoretically calculated deflection values of ordinary concrete beams and foamed concrete beams are in good agreement with the experimental values under normal use conditions, verifying the rationality and effectiveness of the calculation method. The research results of this paper can be taken as a reference for similar engineering designs.

Keywords: prefabricated, plane section assumption, principle of virtual work, lightweight concrete beam

1 Introduction

The prefabricated concrete structure is widely used in building structures. Compared with the traditional cast-in-place structure, the prefabricated concrete structure has diverse advantages, such as short construction periods, high production efficiency, less material consumption, high quality of finished products, low carbon, and environmental protection (Liu et al., 2020; Shah et al., 2021). This structure, however, also has the disadvantage of weak structural integrity (Huang et al., 2021; Savoia et al., 2017), since it is difficult to guarantee the quality of the node construction of prefabricated components. To be specific, the narrow construction environment, high

*Correspondence: rggu@scut.edu.cn
[1] School of Civil Engineering and Transportation, South China University of Technology, Guangzhou 510640, China
Full list of author information is available at the end of the article

Springer Open

© The Author(s) 2022. **Open Access** This article is licensed under a Creative Commons Attribution 4.0 International License, which permits use, sharing, adaptation, distribution and reproduction in any medium or format, as long as you give appropriate credit to the original author(s) and the source, provide a link to the Creative Commons licence, and indicate if changes were made. The images or other third party material in this article are included in the article's Creative Commons licence, unless indicated otherwise in a credit line to the material. If material is not included in the article's Creative Commons licence and your intended use is not permitted by statutory regulation or exceeds the permitted use, you will need to obtain permission directly from the copyright holder. To view a copy of this licence, visit http://creativecommons.org/licenses/by/4.0/.

requirements for construction equipment due to excessive quality of components, the difficulty in the alignment of nodes, and the poor installation accuracy are the key factors affecting the quality of node connections (Chen et al., 2017; Nguyen & Hong, 2020). The adoption of lightweight concrete to reduce the weight of prefabricated components is helpful to solve the above problems. At the same time, this prefabricated component is beneficial to reducing the load of the building structure itself and improving the safety and economy of the building structure. Currently, there are a lot of researches on lightweight concrete, but many lightweight concretes are mainly adopted for functional components. Many scholars have obtained lightweight concrete with significantly improved heat insulation and sound absorption by replacing the aggregates of plain concrete. In recent years, with the deepening of researches, it is promising to utilize some lightweight concrete in structural stress members (Kozłowski & Kadela, 2018; Lee, Kang, et al., 2018; Yang et al., 2016). Many studies explored that the types and contents of lightweight aggregate additions have a great influence on their mechanical properties (Hamidian & Shafigh, 2021; Karamloo et al., 2020; Tian et al., 2020; Vakhshouri & Nejadi, 2018). Therefore, researchers have made a lot of efforts to find the lightweight aggregate concrete that is expected to be used in stressed components.

Although the prefabricated beam functions as one of the main load-bearing components of the prefabricated concrete structure, the research on prefabricated beams made of lightweight concrete is not enough. Lee, Lim, et al. (2018) used lightweight foamed mortar with a 28-day compressive strength of 20 MPa to make reinforced concrete beams, and then conducted bending tests on the beams. Based on the research results, the ultimate load of the reinforced lightweight foam mortar beam was about 8–34% lower than that of plain reinforced concrete with the same steel configuration. However, Jones and McCarthy (2005) once pointed out that most engineers and designers were unlikely to pay much attention to the structural application of foamed concrete unless the strength of foamed concrete exceeds 25 Mpa. Therefore, Lim (2007) conducted bending tests on reinforced foam concrete beams made from 20 to 35 MPa, respectively, and found that both foam concrete beams and ordinary concrete beams showed bending failure models and similar ultimate loads. At the same time, further researches are called upon for beams made of foamed concrete with a compressive strength of 35 Mpa or more. In addition, ceramsite concrete is a type of lightweight concrete that is expected to be used for force members. In recent years, some scholars have studied the bearing capacity and crack width of ceramsite concrete beams. For example, Chen, Li, et al. (2020), Chen, Hui, et al. (2020)) explored the failure mode of shale ceramsite lightweight aggregate concrete beams and the width of diagonal cracks. Moreover, Liu et al (2021) made detailed analysis on the bearing capacity of H-shaped steel beams with circular holes on the webs wrapped in ceramsite concrete (SBWCC) and further proposed a short-term stiffness formula. According to the above researches, it can be found that in the past, the researches on lightweight concrete mainly focused on ultimate strength and ductility. However, flexural members, like beams, should not only have enough strength and ductility but also should meet the service limit state, such as crack width, vibration, and deflection. (Jahami et al., 2019; Wang & Tan, 2021). Nowadays, there are rare studies on the mechanical properties of foamed concrete beams and ceramsite beams with C40 strength grade concrete under normal use conditions. In particular, the mechanical differences between these two types of lightweight concrete beams and plain concrete beams, and the calculation method of the deflection of lightweight concrete beams are rarely explored in the previous studies.

Based on the C60 concrete mix ratio, this study uses lightweight ceramsite or foam material to replace ordinary coarse aggregates so as to obtain a C40 light concrete mix ratio that meets the engineering standards. Besides, ceramsite concrete beams and foamed concrete beams are fabricated. Moreover, through three-point bending tests, this paper further explores the mechanical properties of lightweight concrete beams and plain concrete beams during normal use conditions. Then, the theoretical calculation method of the deflection of the foamed concrete beam is proposed in this paper based on the assumption of flat section and the principle of virtual work. The research results of this paper will help further understand the mechanical properties of lightweight concrete and promote the structural application of lightweight concrete.

2 Experimental Model

2.1 Test Materials and Mix Ratio

This paper intends to explore the mechanical properties of plain concrete, ceramsite concrete, and foamed concrete. Considering that there are many factors that affect the strength of concrete beams, such as the amount of cement, the amount of foam, the amount of ceramsite, the curing conditions, and the water–cement ratio, the compressive strength and flexural strength of the specimens of different materials should meet the minimum engineering requirements in order to better enable the test beam to have sufficient strength to meet engineering requirements. This paper replaces the high-strength concrete with lightweight aggregates to obtain the ratio

of C40 lightweight concrete beams, and then study the mechanical properties of different types of beams. To be specific, referring to the related literature (Chen, Hui, et al., 2020; Chen, Li, et al., 2020; Elrahman Abd, Chung, et al., 2019; Elrahman Abd, Chung, et al., 2019; Gong et al., 2018; Lee et al., 2019; Lotfy et al., 2015; Yu et al., 2013), the author replaced the high-strength C60 concrete coarse aggregate with light aggregates and made standard specimens of compressive and flexural strengths, whose strengths were tested accordingly.

During the whole experiment, Yuexiu brand P·II52.5R cement was used to make lightweight concrete; S95 slag powder with activity index greater than 95% was used for mineral powder, and river sand with a particle size of 2.36 mm or less for fine aggregate The coarse aggregate adopts gravel piles with a bulk density of 1520 kg/m^3 and a particle size of 15 mm or less. In addition, ceramsite with a density of 618 kg/m^3, the cylinder strength of 1.8 Mpa, and the particle size of 8 mm–15 mm and a concentrated high-efficiency cement foaming agent were adopted. In this paper, the types of longitudinally stressed steel bars and stirrup steel bars in the specimens are all HRB500 and HPB300, respectively. The mechanical properties of these steel bars are shown in Table 1.

According to Chinese engineering requirements, the 28d compressive strength of the standard specimens is not less than 40 MPa, and the flexural strength 4.4 MPa. After various trials and tests, a lightweight ceramsite concrete with a 28d compressive strength characteristic value of 41 MPa and a flexural strength characteristic value of 6.62 MPa, and the foamed concrete with 28d compressive strength characteristic value of 41.4 MPa and the characteristic value of flexural strength of 12.97 MPa were prepared. The information of concrete mix ratio is shown in Table 2. The density of plain concrete, the density of foamed concrete, and the density of ceramsite concrete are 2480 kg/m^3, 1900 kg/m^3, and 2000 kg/m^3 respectively. Compared with the density of plain concrete, the density of the two types of lightweight concrete has been reduced by 23.4% and 19.4%, respectively.

Table 1 Mechanical properties of the rebars.

Specimens	f_y (MPa)	f_u (MPa)	E_s (MPa)
HRB500	500	630	2×10^5
HPB300	300	420	2×10^5

2.2 Experimental Design

Considering that T beams have high flexural and shear resistance (Gulec et al., 2021), the cross section of the test beam is designed as a T-section. A total of 5 simply supported beam members were designed and fabricated in the experiment, including 1 plain concrete beam––C, 2 ceramsite concrete beams––CC1 and CC2 (CC1 and CC2 are parallel samples), and 2 foamed concrete beams––FC1 and FC2 (FC1 and FC2 are parallel samples). Since the mid-span bending moment is the largest in the whole beam, the concrete cracks in the tension zone here are most serious and with the fastest speed in the whole beam. Since the strain gage attached to the middle span is prone to fracture, it is specially glued to the 1/4 beam length on the right in order to perform better.

The thickness of the concrete protective layer is 30 mm. According to the Chinese standard, the minimum reinforcement ratio of tensile steel bars is 0.2%, and the reinforcement ratio of tensile steel bars should not exceed 2.5%. In this article, the reinforcement ratio of tension steel bars is 1.9%, and the reinforcement ratio of compression steel bars is 0.4%. The measuring points and reinforcement of the beam are displayed in Fig. 1.

2.3 Loading Scheme

The 3-point bending test is a common method to determine the flexural performance of beams (Bawab et al., 2021; Khatib et al., 2020), and its loading method is simpler than the 4-point bending test (Kyriakopoulos et al.,

Table 2 Concrete mix ratio.

Category	Plain concrete Per m^3	Ceramsite concrete Per m^3	Foamed concrete Per m^3
Cement (kg)	434.0 (18.1%)	434.0 (26.1%)	557.3 (27.9%)
Mineral powder (kg)	144.7 (6.0%)	144.7 (8.7%)	268.3 (13.4%)
Sand (kg)	700.4 (29.2%)	700.4 (42.2%)	990.7 (49.5%)
Water reducing agent (kg)	15.0 (0.6%)	15.0 (0.9%)	18.6 (0.9%)
Water (kg)	138.8 (5.8%)	138.8 (8.4%)	165.1 (8.3%)
Gravel (kg)	967.2 (40.3%)	–	–
Ceramsite (kg)	–	228.5 (13.8%)	–
Foam (L)	–	–	516

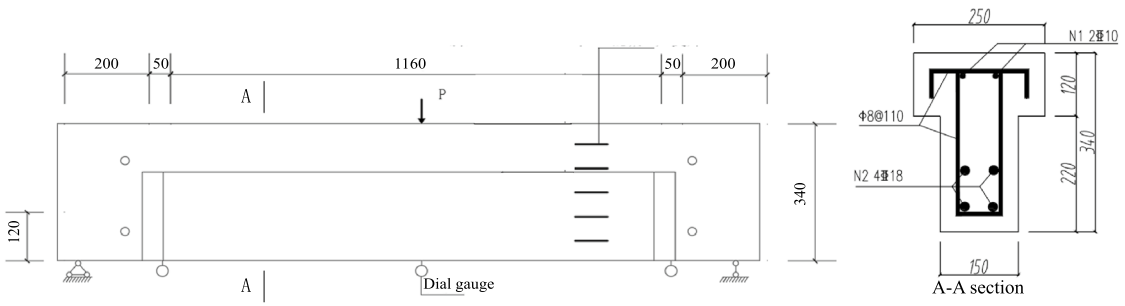

Fig.1 Layout and reinforcement of beam measurement points (unit: mm).

2021; Porter et al., 2019; Xie et al., 2018). Thus, a 3-point bending test was adopted in this study. To verify the reliability and safety of the whole test device, the loading process is divided into preloading and formal loading. The preloading adopts hierarchical loading, with the maximum loading up to 100kN and the loading of each level at 20 kN. After each level of loading is completed, the load is held for 5 min to check whether there is any problem in the entire test system. Hierarchical unloading is performed after the completion of the preloading.

When the preloading is completed, the formal loading is carried out accordingly which is still controlled by load, with a step of 50 kN as the step length. After completing the loading of each level, the load is held for 10 min, and then the corresponding data of each measuring point under the test load of this level are recorded. After loading up to 200 kN, the loading step size is changed to 25 kN so as to better control the sudden occurrence of brittle failure and observe the deformation process of the component in detail.

Apart from having enough strength and ductility, beams should also meet the service limit state (Wang & Tan, 2021). In this context, this test took the service limit into consideration. According to the relevant Chinese standards, the deflection of the flexural member during its service period shall meet a certain limit, which is 1/500 of the calculation span. Therefore, this paper selects the load termination value on the basis of the normal service limit state of the beam. 250 kN was taken as the load termination value by referring to the recommended deflection formula of the Chinese code and the pre-experiments, which means the test ends when the load reaches 250 kN or the ultimate strength of the specimen. Fig. 2 shows the loaded state of specimens.

(a) Experimental T-specimen

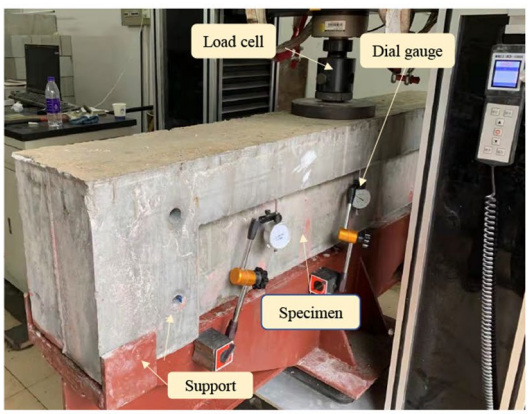

(b) Experimental setup

Fig. 2 Specimen loading. **a** Experimental T-specimen. **b** Experimental setup.

3 Experimental Phenomena and Results

3.1 Experimental Phenomena

The deformation characteristics of foamed concrete and plain concrete are similar throughout the load. When the load reaches about 100 kN, 1–3 vertical cracks in the area near the loading point can be found in the beam. As the load grows, the vertical cracks continue to increase and extend along the height direction and the neutral axis moves upwards. As the load continues, individual

Fig. 3 Destruction of ceramsite concrete beam.

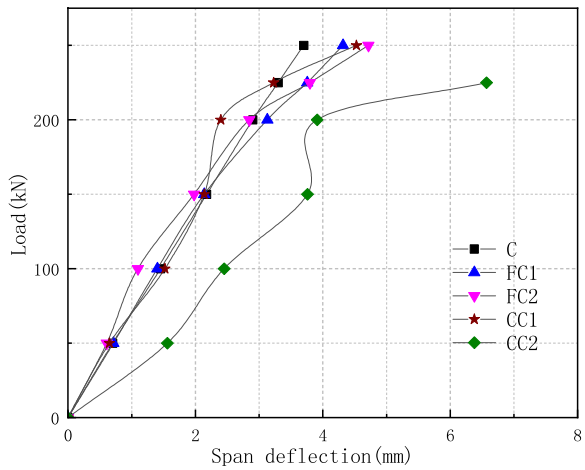

Fig. 4 Load–deflection curve of specimens.

oblique cracks begin to appear at both ends of the beam, and the beam's deflection increases significantly. When continuing the loading, the number of cracks at both ends of the beam shows an upward trend. When the ceramsite concrete beam is loaded to 80 kN, the first vertical crack appears in the middle of the span, and the "click" sound of concrete cracks will be heard. With the continuous loading, it can be found that the number of cracks is more than that of plain concrete beams, and the cracks develop faster. When re-loaded, an oblique crack along the support to the loading point gradually develops. As shown in Fig. 3, when the loading reaches about 225 kN, the specimen suddenly breaks, demonstrating obvious characteristics of shear brittle failure.

3.2 Experimental Results

Fig. 4 shows the load–deflection curve of the specimen. It can be found that at the initial stage of loading, the deflection of each concrete beam increases linearly with the load. With the increase of the load, the beam gradually cracks, the load deflection curve of plain concrete and foamed concrete gradually deviates from the straight line, and the stiffness of the beam decreases. The load deflection data of the two beams of ceramsite concrete are discrete, with the strength significantly lower than that of plain concrete. Since the density of ceramsite (about 600 kg/m^3) is much smaller than that of cement paste (about 1500 kg/m^3), ceramsite tends to float up during concrete solidification, resulting in uneven distribution of ceramsite in concrete. The uneven distribution in concrete, the discreteness of ceramsite strength, and the complexity and randomness of ceramsite interface bonding may lead to the obvious difference of the load deflection data of CC1 and CC2.

4 Calculation of Beam Deflection

Under the load, the section bending moment of the beam member varies along the axis, and the average stiffness or curvature of the corresponding section changes in a complicated way, which is the main reason for accurately calculating the deformation of reinforced concrete members. The direct bilinear method, effective inertia method, and curvature integral method are mainly adopted for the calculation of beam deflection. For example, China's GB 50010-2002 "Concrete Structure Design" adopts the direct bilinear method to calculate the short-term stiffness of components that allow cracks. The American standard ACI 318-99 stipulates that the stiffness calculation after cracking adopts the effective moment of inertia method. In this paper, considering the nonlinear deformation of reinforced concrete beams, the virtual work principle is used to calculate the deflection, and the related calculations are completed with the help of commercial software matlab.

4.1 Basic Assumptions

1) The average strain distribution conforms to the plane section assumption, that is, the average strain of the section is linearly distributed along the height.
2) There is no bond slip between longitudinally tensioned steel bars and concrete. The stress–strain of the longitudinal steel bars adopts an ideal elastoplastic model, and the expression is

$$\begin{cases} \sigma_s = \varepsilon_s E_s, \varepsilon_s \le \varepsilon_y \\ \sigma_s = f_y \ , \varepsilon_y < \varepsilon_s \le \varepsilon_{su} \end{cases}, \quad (1)$$

where σ_s is the steel bar stress, E_s is the steel bar elastic modulus, ε_y is the steel bar yield strain, and f_y is the steel bar yield strength design value.

3) The constitutive models of plain concrete, ceramsite concrete, and foamed concrete are selected with reference to relevant specifications, without considering the tensile effect of concrete. The constitutive model of plain concrete adopts the formula recommended by relevant Chinese standards, and its expression is as follows:

$$\begin{cases} \sigma_c = f_c[1-(1-\frac{\varepsilon_c}{\varepsilon_0})^n], \varepsilon_c \le \varepsilon_0 \\ \sigma_c = f_c \ , \varepsilon_0 < \varepsilon_c \le \varepsilon_{cu} \end{cases}, \tag{2}$$

where σ_c is the concrete stress, f_c is the design value of the concrete compressive strength, ε_0 is the concrete compressive strain when the concrete compressive stress reaches f_c,ε_{cu} is the ultimate compressive strain of the normal section concrete, and n is the coefficient. In this paper, for C40 concrete, ε_0, ε_{cu}, and n are 0.002, 0.0033, and 2.0 respectively.

The constitutive model expressions of ceramsite concrete and foamed concrete are as follows:

$$\begin{cases} \sigma_c = f_c[1.5(\frac{\varepsilon_c}{\varepsilon_0}) - 0.5(\frac{\varepsilon_c}{\varepsilon_0})^2], \ \varepsilon_c \le \varepsilon_0 \\ \sigma_c = f, \qquad\qquad \varepsilon_c > \varepsilon_0 \end{cases} \tag{3}$$

4) The concrete deformation is considered tobe continuous without considering cracks,satisfying the principle of virtual work.

4.2 Bending Analysis and Deflection Calculation of Normal Section

According to the basic assumption of the flat section assumption, the section stress and the strain distribution are shown in Fig. 5 when the properly reinforced beam is in normal service. Assuming that the height of the compression zone of the section is x_c, the strain at the distance y from the neutral axis of the section can be calculated by the assumption of the flat section as follows:

$$\varepsilon(y) = \frac{y}{\rho}. \tag{4}$$

In the formula,ρ is the radius of curvature, and y is the coordinate with the neutral axis as the origin.

According to the force balance condition of the cross section, the following two balance equations can be summarized:

$$\sum X = 0, \int_0^{y_c} \sigma_c(y) \cdot b dy + P_1 + T_1 + T_2 = 0, \tag{5}$$

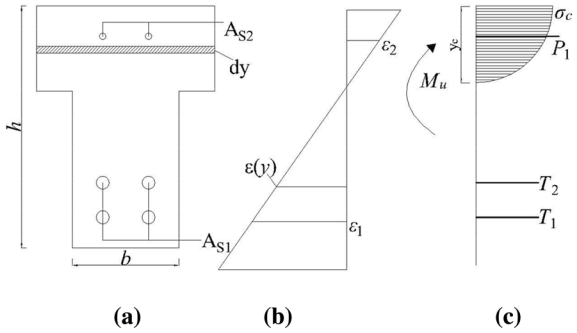

a: T-shaped section section b: Section strain distribution

c: Section stress distribution

Fig.5 Section bending analysis. A_{s1} represents the total area of the tension bars and A_{s2} is the total area of the compression bars. Moreover, ε represents the section strain which is a function of the ordinate. Furthermore, T_1, T_2, and P_1, respectively, represents the resultant force of the first-row tension bars, that of the second-row tension bars, and that of the compressed steel bars. What is more, M_u is the bending moment of section. **a** T-shaped section. **b** Section strain distribution. **c** Section stress distribution

$$\sum M = 0, M_u + \int_0^{y_c} \sigma_c(y) \cdot b \cdot y dy + T_1 y_{t1} + T_2 2 y_{t2} + P_1 y_{p1} = 0, \tag{6}$$

Taking the neutral axis as the origin of the ordinate, upward is positive, and downward is negative; y_{t1}, y_{t2}, and y_{p1}, respectively, represent the ordinate of the resultant force of the first-row tensioned steel bars, that of the second-row tensioned steel bars, and that of compressed steel bars.

From Eqs. (1–6), the relationship between curvature and bending moment can be obtained, and then the curve of deflection and load can be calculated based on the principle of virtual work in Eq. (7). With the increase of load, the neutral axis of the concrete will gradually move up, so the section effective moment of inertia I_e of the concrete will change accordingly, which can be determined by Eq. 8. When using the component, the deformation caused by the axial force and the shear force is negligible. Based on the mathematics software matlab for related programming, this paper calculates the theoretical calculation deflection of each beam by adopting the numerical integration method. In order to ensure sufficient accuracy and calculation speed, the integration step length is selected as 2 mm after multiple debugging.

$$\Delta = \sum \int \frac{\overline{M} M_P}{EIM} \mathrm{ds}, \tag{7}$$

$$I_e = \frac{M_P \rho}{E}, \tag{8}$$

where Δ is the deflection; $\overline{M}$ is the bending moment of the unit load on the virtual beam. M_p is the bending moment of section, and $\rho(M)$ is the corresponding curvature. E is the elastic modulus of reinforced concrete, and I_e is the effective moment of inertia of the section.

5 Results and Analysis

5.1 Load–deflection Curve Analysis

The calculation results are shown in Fig. 6. It can be found that the theoretical calculation values of plain concrete and foamed concrete are in good agreement with the experimental values, the absolute error is mostly within 0.2 mm, and the relative error is mostly 10%–20% during the normal service period. The cracks of the two beams are smaller during the normal service period, which can be calculated based on the virtual work principle with little error. Due to the discreteness of the strength of the ceramsite itself and the uneven distribution of the ceramsite in the concrete, the deflection experimental data of the ceramsite concrete beam are discrete. The crack of ceramsite concrete beam develops rapidly with a large number under the load, and thus, there will be a large error in calculation when using the assumption of plane section and the principle of virtual work.

In order to further verify whether the ceramsite concrete satisfies the plane section assumption, this test measured the concrete strain of the beam under different loads by using strain gages pasted on the side of the ceramsite concrete beam, and further calculated the average strain of the section, so as to obtain the average strain distribution curve of the section. The degree of compliance with the plain section assumption can be found from the curve. Fig. 7 demonstrates the strain distribution of the ceramsite concrete section, in which the strain point at 150 kN and with the section height of 47 mm fails to collect data at this point due to the quality of the strain gage. In addition, the dotted line connection is adopted for the data in this paper. Under lower loads (50 kN, 100 kN), the strain distribution of the cross section of the beam is basically straight at the elastic stage. As the load increases, the section strain begins to deviate from the straight line when the load reaches 150 kN. The section strain is far from the straight line.

5.2 Bending Stiffness

In order to analyze the changes in the bending stiffness of the beam throughout the loading period, the following equation is used for the analysis of the section bending stiffness:

$$B_s = \frac{FL^3}{48\Delta}. \tag{9}$$

As shown in Fig. 8, the bending stiffness of foamed concrete and plain concrete gradually decreases as the load increases. The ceramsite concrete beam has comparatively large discreteness because of the uneven strength of ceramsite, uneven distribution of ceramsite in the beam, and the complexity and randomness of the ceramsite interface and the combination of colloidal materials. Thus, its bending stiffness fluctuates greatly as the load increases. Therefore, through the stiffness trend line

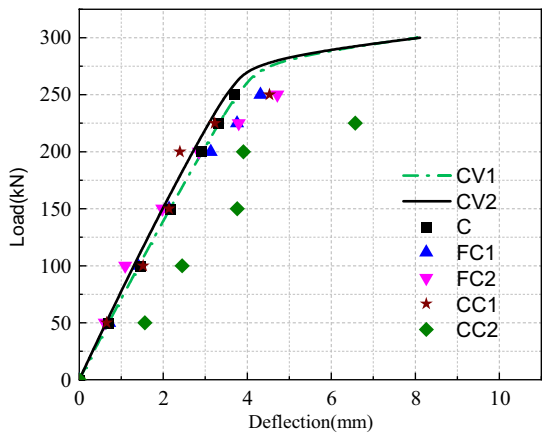

CV1: calculation value of plain concrete beam

CV2: calculation value of light-weight concrete beam

Fig.6 Load deflection of concrete beams. *CV1* calculation value of plain concrete beam, *CV2* calculation value of lightweight concrete beam.

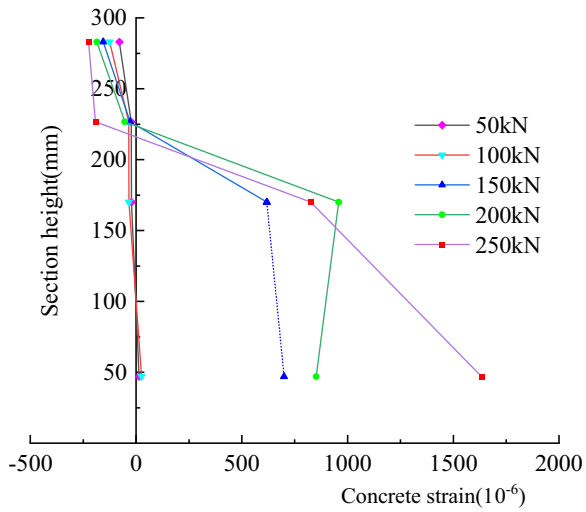

Fig. 7 Distribution of ceramic concrete strain along section height.

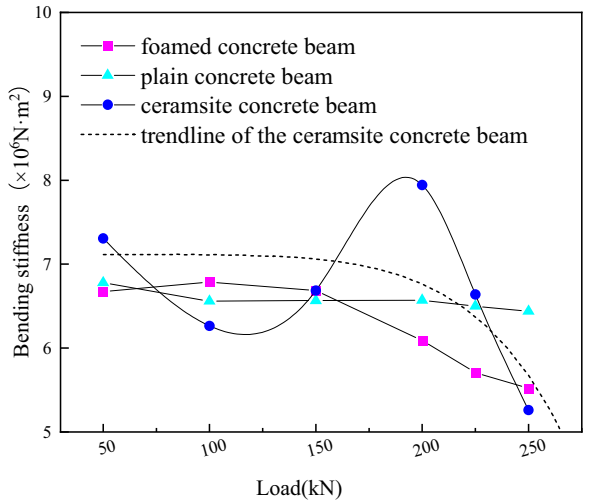

Fig. 8 Bending stiffness of concrete.

of ceramsite concrete beams, the overall change trend of stiffness can be better observed, indicating that the overall trend of stiffness decreases as the load increases.

The deflection of the ceramsite concrete beam decreases rapidly at 100 kN, and the stiffness also plummets. The possible reason is that the ceramsite concrete has some slight cracks during preloading.

The bending rigidity of foamed concrete will decrease with the increase of the load throughout the service period. Table 3 illustrates the bending stiffness of various concrete beams when they reach the normal service limit. When the beam reaches the normal service limit, the bending stiffness of the foamed concrete beam changes by about 10%, and its density is about 23.4% lighter than plain concrete, proving that it is a very good lightweight concrete. The material properties and uneven distribution of ceramsite concrete have a greater impact on the test results, so further research is needed.

5.3 Failure Analysis

As shown in Table 4, in the experiment, the foamed concrete beam failed due to the deflection reaching the service limit, and the ceramsite concrete beam suddenly broke with the development of the shear crack. The ceramsite concrete suffers brittle shear failure at 225 kN, demonstrating that its bearing capacity is significantly lower than that of plain concrete. The strength of the coarse aggregate in plain concrete is higher than the strength of the interface between the cement base stone and the coarse aggregate (Xiao et al., 2013), so the failure of concrete generally starts from the interface. However, the strength of ceramsite is relatively lower than that of the cement base and the interface, so the failure of the ceramsite concrete beam is caused by the cracking of the coarse aggregate of the ceramsite concrete beam until it penetrates the entire oblique section. The phenomena are consistent with the opinion proposed by Zhang and Gjvorv (1991) that aggregate strength is the main factor affecting the strength of lightweight aggregate concrete.

Table 4 Experimental results of the lightweight beam

	Foamed concrete beam	Ceramsite concrete beam
μ_r	1.13	0.94
Energy absorption ratio	1.03	0.92
Failure mode	Service limit	Shear crack

5.4 Displacement Ductility and Energy Absorption

Ductility is often used to represent a structure's ability to resist inelastic behavior. Based on the previous literature, there are a variety of calculation models for calculating displacement ductility factors. Park mode (Gulec et al., 2021; Park., 1988) is a commonly used model for calculating ductility factor, which is the ratio of failure point displacement to yield point displacement (Khatib et al., 2020). By referring to the Park model and the service limit requirements of the beam, this paper defines the displacement factor (μ) as the ratio of the service displacement value (Δu) of the beam to the corresponding equivalent elastoplastic yield point displacement (Δy)

Table 3 Limit bending stiffness.

	Plain concrete	Foamed concrete	Ceramsite concrete
Deflection limit (mm)	3.16	3.16	3.16
The corresponding load of deflection limit(kN)	216.3	201.2	222.9
Bending stiffness (10^6 N·m^2)	6.52	5.88	6.75
Initial bending stiffness (10^6 N·m^2)	6.78	6.67	7.31
Rate of change	3.83%	11.84%	7.70%

The initial bending stiffness represents the bending stiffness of 50kN.

(Eq. 10). In order to compare the ductility of the lightweight concrete beams and plain concrete beams, the relative ductility ratio u_r is further defined as Eq. 11.

$$\mu = \frac{\Delta_u}{\Delta_y}, \tag{10}$$

$$\mu_r = \frac{\mu_l}{\mu_p}, \tag{11}$$

where μ_l and $\mu_{p,}$ respectively, represent the ductility factor of lightweight concrete beams and that of the plain concrete beams.

The average values of the relative ductility ratio of these two kinds of lightweight concrete beams are shown in Table 4. As shown in the table, compared with the plain concrete beam, the ductility of foamed concrete beams is 1.13 times of the plain concrete beam's ductility, demonstrating that foamed concrete beam has higher ductility. However, the ductility of the ceramsite concrete beam is slightly lower than that of the plain concrete beam, which indicates that replacing coarse aggregate with ceramsite will reduce the quality of the beam but lead to a reduction in the ductility of the beam.

The energy absorption capacity of the beam can be used to reflect the resistance ability to inelastic deformation. The energy absorption capacity of the beam can be obtained by calculating the area under the force–displacement curve (Gulec et al., 2021), which can be obtained by the sum of the area of two successive points (Eq. 12):

$$\text{Energy absorption} = 0.5\sum_{i=1}^{n-1}(d_{i+1}-d_{\mathrm{i}})(F_{i+1}-F_i), \tag{12}$$

where d_i represents the displacement; F_i represents the load (kN) at this displacement (mm); n represents the number of displacement points.

The energy absorption ratio is defined as the ratio of the absorbed energy of lightweight concrete beams to that of plain concrete to compare the energy absorption of lightweight concrete beams and plain concrete beams. The average energy absorption of lightweight concrete beams is shown in Table 4. It can be found that the energy absorption capacity of the ceramsite concrete beam is the lowest in all beams, while the energy absorption capacity of the foam concrete beam is 3% higher than that of the plain concrete beam.

6 Conclusion

The paper obtains the mix ratio of lightweight concrete by replacing the coarse aggregate of high-strength concrete with lightweight ceramsite or foam based on the C60 concrete mix ratio. After that, lightweight concrete beams are fabricated and three-point bending tests are carried out. Through the experiments and theoretical analysis, the following conclusions can be drawn from the results of this study.

(1) The mechanical properties of C40 foam concrete beams are similar to those of plain concrete beams. Compared to plain concrete beams, the density of foamed concrete was lower by 23.4%; moreover, the ductility and toughness of foamed concrete were higher by 13 and 3%, respectively.
(2) Considering the nonlinear deformation characteristics of reinforced concrete beams, the theoretical calculation method of beam deflection is proposed based on the flat section assumption and the principle of virtual work. Within the normal use deflection limits, the calculated results are in good agreement with the deflection of plain concrete beams and foam concrete beams, the absolute error is mostly within 0.2 mm, and the relative error is mostly 10–20% during the normal service period, verifying that the calculated value can be used as a design reference for the deflection of the foamed concrete beam during normal use.
(3) The mechanical properties of C40 ceramsite concrete beam have comparatively large discreteness. This may be caused by the strength discreteness of the ceramsite, the uneven distribution of ceramsite in the concrete beam, and the complexity and randomness of the combination of ceramsite interface and colloid. Thus, the aforementioned points should be attached great importance to in subsequent research and design.

Acknowledgements

This work was financially supported by the National Key Scientific Instruments and Equipment Development Projects of China(Grant No. 41827807), the Open Research Fund of the State Key Laboratory of Geomechanics and Geotechnical Engineering, Institute of Rock and Soil Mechanics, Chinese Academy of Sciences (Grant No. Z018019), the State Key Laboratory of Subtropical Building Science in China(Grant No. 2017KB16), and Guangdong Provincial Key Laboratory of Modern Civil Engineering Technology in China (Grant No. 2021B1212040003).

Authors' contributions

YF contributed to supervision and project administration. YX was involved in writing the manuscript. RG was responsible for the method design

and revising the manuscript. All the authors read and approved the final manuscript.

Authors' information
Yingguang Fang is a Professor of Civil Engineering at South China University of Technology.
Yafei Xu is a graduate student in School of Civil Engineering and Transportation, South China University of Technology.
Renguo Gu is an Associate Professor of Civil Engineering at South China University of Technology.

Funding
National Key Scientific Instrument and Equipment Development Projects of China, 41827807, Yingguang Fang, Institute of Rock and Soil Mechanics, Chinese Academy of Sciences, Z018019, Renguo Gu, the State Key Laboratory of Subtropical Building Science in China, 2017KB16, and Renguo Gu, Guangdong Provincial Key Laboratory of Modern Civil Engineering Technology in China, 2021B1212040003.

Availability of data and materials
The data and materials used to support the findings of this study are available from the corresponding author upon request.

Declarations

Competing interests
The authors declare that they have no competing interests.

Author details
[1]School of Civil Engineering and Transportation, South China University of Technology, Guangzhou 510640, China. [2]State Key Laboratory of Subtropical Architectural Science, Guangzhou 510640, China.

Received: 8 June 2021 Accepted: 25 December 2021
Published online: 14 January 2022

References

Bawab, J., Khatib, J., Jahami, A., Elkordi, A., & Ghorbel, E. (2021). Structural Performance of Reinforced Concrete Beams Incorporating Cathode-Ray Tube (CRT) Glass Waste. *Buildings, 11*(2), 67.
Chen, M., Li, Z., Wu, J., et al. (2020). Shear behaviour and diagonal crack checking of shale ceramsite lightweight aggregate concrete beams with high-strength steel bars. *Construction and Building Materials., 249*, 118730.
Chen, Y., Hui, Q., Zhang, H., Zhu, Z., & Wang, C. (2020). Experiment and application of ceramsite concrete used to maintain roadway in coal mine. *Measurement and Control., 53*, 1832–1840.
Chen, Z., Liu, J., & Yu, Y. (2017). Experimental study on interior connections in modular steel buildings. *Engineering Structures, 147*, 625–638.
Elrahman Abd, M., Chung, S., & Stephan, D. (2019). Effect of different expanded aggregates on the properties of lightweight concrete. *Magazine of Concrete Research., 71*, 95–107.
Elrahman Abd, M., Madawy El, M., Chung, S., Sikora, P., & Stephan, D. (2019). Preparation and characterization of ultra-lightweight foamed concrete incorporating lightweight aggregates. *Applied Sciences., 9*, 1447.
Gong, J., Zeng, W., & Zhang, W. (2018). Influence of shrinkage-reducing agent and polypropylene fiber on shrinkage of ceramsite concrete. *Construction and Building Materials., 159*, 155–163.
Gulec, A., Kose, M. M., & Gogus, M. T. (2021). Experimental investigation of flexural performance of T-section prefabricated cage reinforced beams with self-compacting concrete. *Structures*. https://doi.org/10.1016/j.istruc.2021.05.074
Hamidian, M. R., & Shafigh, P. (2021). Post-peak behaviour of composite column using a ductile lightweight aggregate concrete. *International Journal of Concrete Structures and Materials*. https://doi.org/10.1186/s40069-020-00453-6
Huang, W., Hu, G., Miao, X., & Fan, Z. (2021). Seismic performance analysis of a novel demountable precast concrete beam-column connection with multi-slit devices. *Journal of Building Engineering, 44*, 102663.
Jahami, A., Khatib, J., Baalbaki, O., & Sonebi, M. (2019). Prediction of deflection in reinforced concrete beams containing plastic waste. *SSRN J.* https://doi.org/10.2139/ssrn.3510113
Jones, M. R., & McCarthy, A. (2005). Preliminary views on the potential of foamed concrete as a structural material. *Magazine of Concrete Research, 57*(1), 21–31.
Karamloo, M., Afzali-Naniz, O., & Doostmohamadi, A. (2020). Impact of using different amounts of polyolefin macro fibers on fracture behavior, size effect, and mechanical properties of self-compacting lightweight concrete. *Construction and Building Materials., 250*, 118856.
Khatib, J. M., Jahami, A., Elkordi, A., Abdelgader, H., & Sonebi, M. (2020). Structural assessment of reinforced concrete beams incorporating waste plastic straws. *Environments, 7*(11), 96.
Kozłowski, M., & Kadela, M. (2018). Mechanical characterization of lightweight foamed concrete. *Advances in Materials Science & Engineering., 2018*, 1–8.
Kyriakopoulos, P., Peltonen, S., Vayas, I., Spyrakos, C., & Leskela, M. V. (2021). Experimental and numerical investigation of the flexural behavior of shallow floor composite beams. *Engineering Structures, 231*, 111734.
Lee, J., Kang, S., Ha, Y., & Hong, S. (2018). Structural behavior of durable composite sandwich panels with high performance expanded polystyrene concrete. *International Journal of Concrete Structures and Materials*. https://doi.org/10.1186/s40069-018-0255-6
Lee, Y. L., Lim, J. H., Lim, S. K., & Tan, C. S. (2018). Flexural behaviour of reinforced lightweight foamed mortar beams and slabs. *KSCE Journal of Civil Engineering, 22*(8), 2880–2889.
Lee, K., Yang, K., Mun, J., & Tuan, N. (2019). Effect of sand content on the workability and mechanical properties of concrete using bottom ash and dredged soil-based artificial lightweight aggregates. *International Journal of Concrete Structures and Materials*. https://doi.org/10.1186/s40069-018-0306-z
Lim, H. (2007). *Structural response of LWC beams in flexure*. National University of Singapore.
Liu, X., Meng, K., Zhang, A., Zhu, T., & Yu, C. (2021). Bearing capacity of H-section beam wrapped with ceramsite concrete. *Steel and Composite Structures, 40*(5), 679–696.
Liu, Y., Ma, H., Li, Z., & Wang, W. (2020). Seismic behaviour of full-scale prefabricated RC beam–CFST column joints connected by reinforcement coupling sleeves. *Structures*. https://doi.org/10.1016/j.istruc.2020.10.066
Lotfy, A., Hossain, K. M. A., & Lachemi, M. (2015). Lightweight self-consolidating concrete with expanded shale aggregates, modelling and optimization. *International Journal of Concrete Structures and Materials., 9*, 185–206.
Nguyen, D. H., & Hong, W. K. (2020). A novel erection technique of the L-shaped precast frames utilizing laminated metal plates. *Journal of Asian Architecture and Building Engineering*. https://doi.org/10.1080/13467581.2020.1841644
Park, R. (1988) Ductility evaluation from laboratory and analytical testing. *Proceedings of the 9th world conference on earthquake engineering, Tokyo-Kyoto, Japan*. Vol. 8.
Porter, J. H., Cain, T. M., Fox, S. L., & Harvey, P. S. (2019). Influence of infill properties on flexural rigidity of 3D-printed structural members. *Virtual and Physical Prototyping, 14*(2), 148–159.
Savoia, M., Buratti, N., & Vincenzi, L. (2017). Damage and collapses in industrial precast buildings after the 2012 Emilia earthquake. *Engineering Structures, 137*, 162–180.
Shah, Y. I., Hu, Z., Yin, B. S., & Li, X. (2021). Flexural performance analysis of UHPC wet joint of prefabricated bridge deck. *Arabian Journal for Science and Engineering*. https://doi.org/10.1007/s13369-021-05735-z
Tian, Y., Yan, X., Zhang, M., Yang, T., & Zhang, J. (2020). Effect of the characteristics of lightweight aggregates presaturated polymer emulsion on the mechanical and damping properties of concrete. *Construction and Building Materials., 253*, 119154.
Vakhshouri, B., & Nejadi, S. (2018). Size effect and age factor in mechanical properties of BST Light Weight Concrete. *Construction and Building Materials, 177*, 63–71.

Wang, S., & Tan, K. H. (2021). Flexural performance of reinforced carbon nanofibers enhanced lightweight cementitious composite (CNF-LCC) beams. *Engineering Structures, 238*, 112221.
Xiao, J., Li, W., Corr, D. J., & Shah, S. P. (2013). Effects of interfacial transition zones on the stress–strain behavior of modeled recycled aggregate concrete. *Cement and Concrete Research, 52*, 82–99.
Xie, J., Huang, L., Guo, Y., Li, Z., Fang, C., Li, L., & Wang, J. (2018). Experimental study on the compressive and flexural behaviour of recycled aggregate concrete modified with silica fume and fibres. *Construction and Building Materials, 178*, 612–623.
Yang, K. H., Lee, Y., & Joo, D. B. (2016). Flexural behavior of post-tensioned lightweight concrete continuous one-way slabs. *International Journal of Concrete Structures and Materials, 10*(4), 425–434.
Yu, X. Q., Lin, M., Geng, G. L., Li, Y. H., & Jia, L. (2013). Preparation test study on High strength lightweight concrete in engineering materials. *Advanced Materials Research*. https://doi.org/10.4028/www.scientific.net/AMR.648.55
Zhang, M. H., & Gjvorv, O. E. (1991). Mechanical properties of high-strength lightweight concrete. *Materials Journal, 88*(3), 240–247.

Publisher's Note

Springer Nature remains neutral with regard to jurisdictional claims in published maps and institutional affiliations.

Submit your manuscript to a SpringerOpen journal and benefit from:

► Convenient online submission
► Rigorous peer review
► Open access: articles freely available online
► High visibility within the field
► Retaining the copyright to your article

Submit your next manuscript at ► springeropen.com